


# Sowmi Sathiya

## RE-2022-481731.doc

 Peninsula College

---

### Document Details

**Submission ID****trn:oid::27450:82724077****Submission Date****Feb 20, 2025, 12:21 AM GMT+5:30****Download Date****Feb 20, 2025, 12:26 AM GMT+5:30****File Name****RE-2022-481731.doc****File Size****1.5 MB****7 Pages****3,751 Words****22,956 Characters**





# 10% Overall Similarity

The combined total of all matches, including overlapping sources, for each database.




## Filtered from the Report

- Bibliography
- Quoted Text

## Match Groups

-  **26 Not Cited or Quoted 10%**  
Matches with neither in-text citation nor quotation marks
-  **0 Missing Quotations 0%**  
Matches that are still very similar to source material
-  **0 Missing Citation 0%**  
Matches that have quotation marks, but no in-text citation
-  **0 Cited and Quoted 0%**  
Matches with in-text citation present, but no quotation marks

## Top Sources

- 7%  Internet sources
- 6%  Publications
- 6%  Submitted works (Student Papers)

## Integrity Flags

### 0 Integrity Flags for Review

No suspicious text manipulations found.

Our system's algorithms look deeply at a document for any inconsistencies that would set it apart from a normal submission. If we notice something strange, we flag it for you to review.

A Flag is not necessarily an indicator of a problem. However, we'd recommend you focus your attention there for further review.

## Match Groups

- 26 Not Cited or Quoted 10%**  
Matches with neither in-text citation nor quotation marks
- 0 Missing Quotations 0%**  
Matches that are still very similar to source material
- 0 Missing Citation 0%**  
Matches that have quotation marks, but no in-text citation
- 0 Cited and Quoted 0%**  
Matches with in-text citation present, but no quotation marks

## Top Sources

- 7% Internet sources
- 6% Publications
- 6% Submitted works (Student Papers)

## Top Sources

The sources with the highest number of matches within the submission. Overlapping sources will not be displayed.

1	Internet	www.rcciit.org	3%
2	Internet	www.philstat.org	2%
3	Publication	Xuan Jiang, Tong Shen, Mingjie Tan, Jianlin Wang. "Research on Seismic Wave Firs...	<1%
4	Submitted works	Universitas Dian Nuswantoro on 2025-02-19	<1%
5	Submitted works	Southern New Hampshire University - Continuing Education on 2022-06-10	<1%
6	Internet	portfolio.vvsu.ru	<1%
7	Internet	w3.cran.univ-lorraine.fr	<1%
8	Publication	"Advances in Deep Generative Models for Medical Artificial Intelligence", Springe...	<1%
9	Submitted works	Taylor's Education Group on 2025-01-10	<1%
10	Publication	"Machine Learning in Medical Imaging", Springer Science and Business Media LL...	<1%

11	Publication	Daniele Peila, Giulia Viggiani, Tarcisio Celestino. "Tunnels and Underground Citie...	<1%
12	Internet	dokumen.pub	<1%
13	Internet	www.arxiv-vanity.com	<1%
14	Internet	www.healthoma.com	<1%
15	Publication	H.L. Gururaj, Francesco Flammini, S. Srividhya, M.L. Chayadevi, Sheba Selvam. "Co...	<1%

# A DEEP LEARNING APPROACH FOR CLASSIFICATION OF CANCER FROM CT/MRI IMAGES

Nirmalrani V<sup>1</sup>

Department of Computer Science and Engineering, Sathyabama Institute of Science and Technology,  
Chennai, India

[nirmalrani.it@sathyabama.ac.in](mailto:nirmalrani.it@sathyabama.ac.in)

Hari Shankar S<sup>3</sup>

Department of Computer Science and Engineering, Sathyabama Institute of Science and Technology,  
Chennai, India

[harishankar2003.25@gmail.com](mailto:harishankar2003.25@gmail.com)

K L Haresh Ragavender <sup>2</sup>

Department of Computer Science and Engineering, Sathyabama Institute of Science and Technology,  
Chennai, India

[hareshkl04@gmail.com](mailto:hareshkl04@gmail.com)

Viveha R<sup>4</sup>

Department of Computer Science and Engineering, Sathyabama Institute of Science and Technology,  
Chennai, India

[Vrviveha@gmail.com](mailto:Vrviveha@gmail.com)

**Abstract**—Medical imaging technology developments have raised the standard of both cancer detection and treatment preparation capabilities. The accurate identification of several cancer types within CT/MRI imaging data proves to be a complex medical diagnostic problem. The research adopts InceptionV3 and EfficientNet-B7 deep learning architectures to develop a new cancer classification system. Diagnosis performance and precision stand as the main targets for this research. Our research design includes acquiring a wide-ranging set of CT/MRI images which show different breast, kidney and brain cancer manifestations. The system utilizes modern convolutional neural networks (CNNs) to obtain relevant information from medical images. The medical field requires this research because the advanced cancer classification tool enables better decisions and tailored treatment planning for breast and kidney and brain cancer patients. The proposed method demonstrates potential to enhance both patient care and progress within medical imaging exploration for cancer identification.

**Keywords**— Breast cancer, Kidney cancer, Brain cancer, Convolutional neural networks (CNNs), Medical imaging, Cancer classification, Deep learning

## I. INTRODUCTION

Artificial intelligence (AI) contains different technologies which use computers to mimic human intelligence. The artificial intelligence method called Deep learning functions through neural network algorithms that were built using brain-inspired neurological designs. DL achieves exponential scalability through neural networks as a result of not following the traditional logistic regression approach used in traditional ML methods. DL represents an invaluable tool for dealing with complex computational problems including massive image recognition along with natural language processing and speech recognition and language translation.

Borderline cancer treatment shifts towards specific treatment approaches through the combination of various data types which include genomic data together with transcriptomic analysis and pathologic data. The integration process requires more extensive resources than single data interpretation thus it demands learning models that can extract valuable information from complex features.

The healthcare approach for cancer treatment changes towards specific care through an integrated analysis framework that combines genomic information with transcriptomic and histopathologic results. The integration process requires more extensive resources than single data interpretation thus it demands learning models that can extract valuable information from complex features.

A transformation occurs in cancer care through precision healthcare models that unite genomic and transcriptomic and histopathologic data types. The integration process requires more extensive resources than single data interpretation thus it demands learning models that can extract valuable information from complex features.

Medical care for cancer patients progresses towards specific healthcare through tools that unify multiple data kinds including genetic and cell expression sequences and tissue examination information. The integration process requires more extensive resources than single data interpretation thus it demands learning models that can extract valuable information from complex features.

The field of cancer care is making its shift towards precise healthcare through the combination of genomic and transcriptomic and histopathologic data. The integration process requires more extensive resources than single data interpretation thus it demands learning models that can extract valuable information from complex features.

The collection evaluates methods that assist researchers working on deep learning for multimodal medical imaging. The objective of this initiative focuses on encouraging researchers to present their best work because this step propels future innovation in this field.

## II. LITERATURE REVIEW

A review of transfer learning for classification and regression and clustering problems appeared in the published research of Pan and Yang [5]. The authors studied in this survey how transfer learning connects with domain adaptation, multitask learning and sample selection bias and co-variate shift techniques in machine learning. The researchers also investigated upcoming matters within transfer learning research. The researchers reviewed multiple existing trends in transfer learning through this survey piece.

A Survey on Brain Tumor Detection Using Image Processing Techniques by Luxit Kapoor, Sanjeev [6]. Medical Image Processing includes multiple techniques which experts use to discover brain tumors in MRI Images according to this paper. The research findings became the basis for writing this Paper where different detection approaches are listed. The text includes descriptions of all techniques with brief explanations. Segmentation stands as the most important step among all processes leading to tumor detection..

According to S. Banerjee, S.Mitra, and B.U. Shankar [7] seven standard classifiers achieved their accuracy rates on BRaTS 2015 dataset through evaluation methods such as i) Adaptive Neuro- Fuzzy Classifier (ANFC), ii) Naive Bayes(NB), iii) Logistic Regression (LR), iv) Multilayer Perceptron(MLP), v) Support Vector Machine (SVM), vi) Classification and Regression Tree (CART), and vii) k-nearest neighbours (k-NN). The evaluation of classifier performance occurs through analysis of BRaTS 2015 dataset (a subset of BRaTS 2017 dataset) which includes 200 HGG and 54 LGG cases. Researchers extracted 56 three-dimensional quantitative MRI features manually from each patient MRI as input for classification.

The performance results of the study led the authors to create ChurnNet [9] as a deep learning architecture which integrates 1D convolutional elements and attention modules with residual blocks. The modified model demonstrated increased accuracy for predicting customer attrition in telecom businesses over previous predictive structures.

The authors Lee et al. (2021) [10] developed a hybrid technique combining statistical and machine learning predictive methods for minimizing churn prediction misclassification errors which proved effective across different sectors with minimal required data.

Random Forest algorithm received enhancements from Al-Sultan and Al-Baltah [11] to enhance banking sector churn prediction capabilities especially in handling unbalanced datasets thereby directing banks to deploy

smarter retention approaches. Researchers Z. Shi et al. [12] created D-CNNs which integrate spatial and frequency-domain CNNs with a preprocessing layer to identify tampered areas resulting in high F1 scores on different datasets.

T. The research of Min-Jen in collaboration with C. Cheng-Tao [13] introduces DC-CNN to detect GAN-based deepfake palmprints while achieving detection accuracy surpassing 90% for WGAN fakes. S. A. MMGANGuard represents a scalable ensemble detection system for deepfakes which tackles traditional forensic method limitations according to S. A. Raza et al. [14]. S. The paper by Safwat et al. [15] evaluates ML and DL techniques for fake content detection while discussing adversarial attacks together with forthcoming research directions.

## III.METHODOLOGY

The paper approaches modern medical diagnostics by introducing a reliable methodology which classifies different types of lung kidney and brain cancers automatically through deep learning architecture integration of CNN/InceptionV3 and EfficientNetB3. The preprocessed dataset consisting of medical images contains diverse examples which are partitioned into training, validation and test sets after data augmentation. The implementation of transfer learning starts with pre-trained weights from ImageNet datasets that are applied to the networks followed by freezing the initial layers to preserve low-level features. The final layer structures of the networks require adjustment to perform the multi-cancer diagnosis operation.

An appropriate training process uses the cancer dataset as part of the fine-tuning procedure while employing proper optimizers alongside loss functions. The process of evaluation includes testing on specific data sets so performance metrics can be measured. The process of adjusting parameters known as hyperparameters leads to improved learning rates together with better batch sizes. Results are studied through confusion matrices together with visual displays which provide information about how the model operates. The research supports the integration process of leading deep learning methods into medical diagnostics as it explores superior architectures for multi-cancer identification. Research experiments lead to the selection of the top strategy for cancer classification among the examined architectures. The research adds substantial progress to medical diagnostic technology by investigating the most effective deep learning techniques for multi-cancer classification.

### A. Data Collection

### BRaTS MICCAI dataset:

The collection includes 220 HGG patients and 27 LGG patients as demonstrated in fig:1. A total of 110 brain images belonging to HGG and LGG patients exist in the \_test\_ directory. Each patient receives a total of five MRI image modalities named T1, T2, T1C, FLAIR and OT (Ground truth of tumor Segmentation). This dataset contains five MRI image modalities which store their files as .mha format at 240x240 resolution and each image uses (1 mm<sup>3</sup>) voxel size and skull- stripping. The ground truth images contain numerical voxel labels that distinguish normal pixels from tumor cell sections by representing normal pixels with zero values and tumor cell parts with non-zero values.

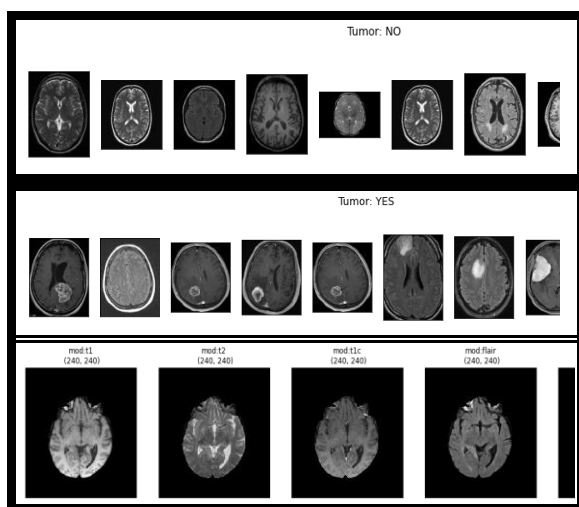


Fig: 1. MICCAI dataset

### Kidney dataset:

In fig:2 images from this class show the anatomy or organ appearing normally as it should in healthy state along with no pathological issues. The body produces fluid-filled sacs known as cysts which appear throughout its different areas. The images contained in this class visualize cysts that appear in the observed organs and regions. Images that show tumor appearance are most likely included within this class. Tissue mass differences known as tumors occur both as benign non-cancerous growths and malignant cancerous growths. Different types of tumors can be found within the images of this class. Calculi with their mineral and salt accumulated composition are called stones which appear throughout various areas of the human body including kidney stones and gallstones. This picture class shows any stones located within the examined organ or system.

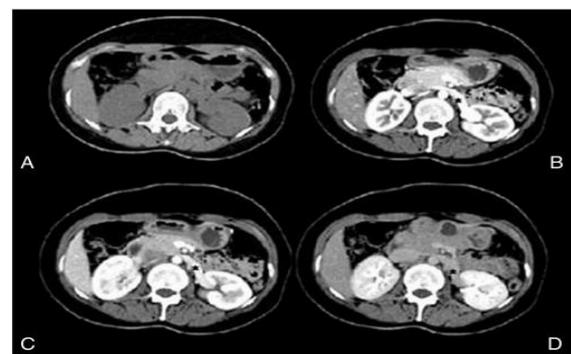


Fig: 2. Kidney dataset

Lung Cancer dataset: The Lung Cancer dataset presents NSCLC along with Adenocarcinoma types and Squamous cell carcinoma and Large cell (undifferentiated) carcinoma in fig:3.

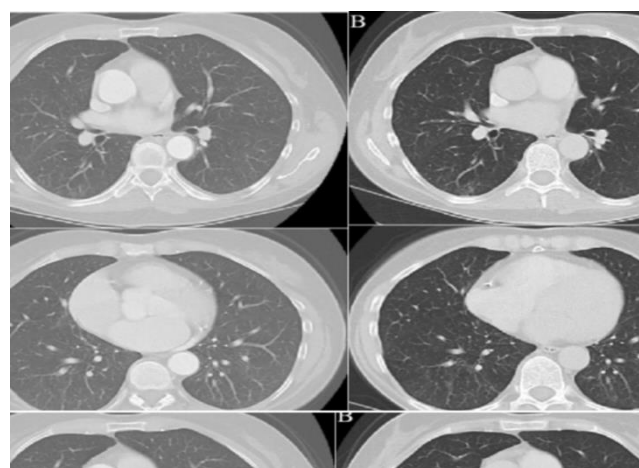


Fig.3.Lung cancer

### B. Data Preprocessing

The initial stage of data readjustment holds crucial importance for making data ready to use with deep learning models specifically designed for image classification purposes. Alongside preprocessing methods we apply data augmentation methods that include shearing, zooming and horizontal flipping. The various augmentations create multiple image perspectives which help the model acquire generalized performance across different spatial configurations as well as varying orientations.

Here are some common data augmentation techniques:

Users can utilize two functions to modify images: they can horizontally or vertically flip images and rotate them through different angle degrees. Through this approach the model gains ability to recognize objects in different positional variations. During the process users can select portions of the image before either enlarging or decreasing their size or performing random cropping operations. By doing



11 this the model develops resistance to different object positions and size variations.

Random adjustments of brightness and contrast levels exist as part of this technique. The model develops greater sensitivity to various lighting conditions through this technique. The model operates images through two ways: scaling transforms images to different dimensions while shearing modifies their visual perspective. The model develops generalized ability to identify objects with various forms through this training process.

15 Noise Injection: Adding random noise serves as an addition to image modification during training. The model develops improved durability against erroneous input through this technique. A random modification process affects the color channels found in images through Color Jittering. Such form of augmentation allows the model to develop better capabilities for processing distinct color distribution patterns.

2 Elastic Distortions: The image requires various types of random deformation for this process. Through this technique the model develops stronger immunity to input data variations. Random Erasing involves applying random noise in place of removing random image sections throughout the image. It keeps the model from fixing itself on learning specific patterns.

Data augmentation serves its purpose best when the training dataset remains small. The model gains exposure to a multitude of situations by producing varied versions of already existing data. Such techniques protect against overfitting behavior thereby enhancing performance on new data and evaluation scenarios.

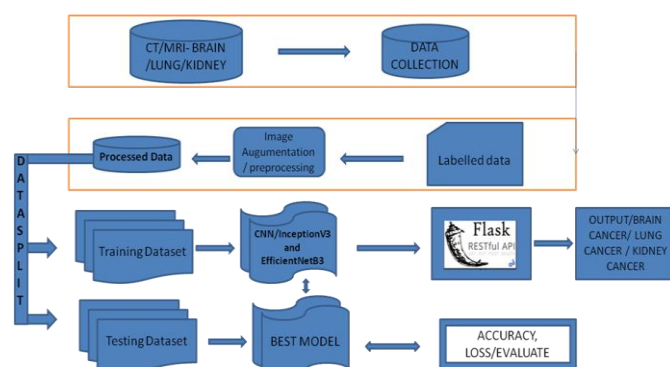


Fig.4. Block Diagram

### C. Model Training

The process of training models illustrated in fig:4 includes systematic work steps for the deep learning approaches CNN, InceptionV3 and EfficientNetB3 to optimize parameter settings for accurate multi cancer identification.

### 1. CNN

The Convolutional Neural Network (CNN) serves as a deep learning neural architecture for Medical Imaging multi-cancer prediction tasks as represented in fig:5. It contains multiple layers.

**Input Layers:** The input layer maintains the number of features that feed into our model. This layer contains a number of neurons matching the exact count of features we provide (pixel count in image data).

**Hidden Layer:** The received information from the Input layer moves forward into the hidden layer. Different hidden layer combinations will form part of our model based on its size and data requirements. The number of neurons in each concealed layer varies across different layers although they often exceed the number of input features. Each layer calculates its output through weight matrix multiplication starting from the previous layer results along with bias addition before running it through an activation function to create nonlinear relations.

**Output Layer:** Hidden layer output proceeds to the logistic function sigmoid or softmax for conversion into probability scores of individual classes.

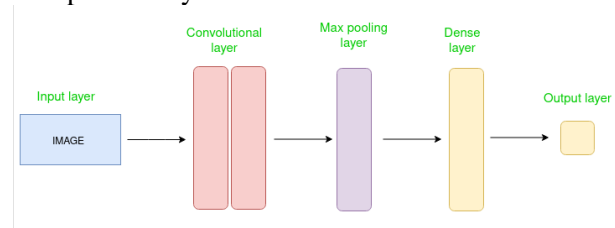


Fig :5 CNN architecture

### 2. EfficientNet-B3

The convolutional neural network architecture and scaling method known as EfficientNet in fig:6 uses a compound coefficient for uniform scaling of network dimensions including depth/width/resolution. The EfficientNet approach conducts uniform scaling of network factors such as depth and resolution as well as width through established scaling coefficients.

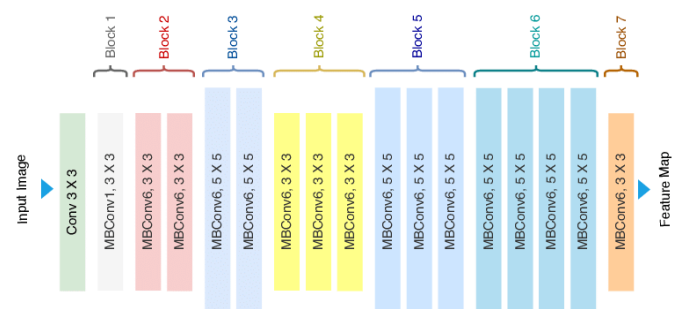


Fig.6. EfficientNet-B3



The base unit for EfficientNet-B3 architecture is the mobile inverted bottleneck MBConv block which serves as the inverted residual structure with an added SE (Squeeze and Excitation) block. The following description covers the two blocks of architecture.

Platform EfficientNet-B7 received the compound scaling approach as its foundation. They established a constant value of  $\Phi=1$  as they executed a search through parameter combinations of  $\alpha, \beta$  and  $\gamma$  using the provided mathematical equations subject to the condition that  $\alpha \cdot \beta^2 \cdot \gamma^2 \approx 2$ . The found values for the different parameters included  $\alpha=1.2$  while  $\beta=1.1$  and  $\gamma=1.15$ .

### 3.Inception V3

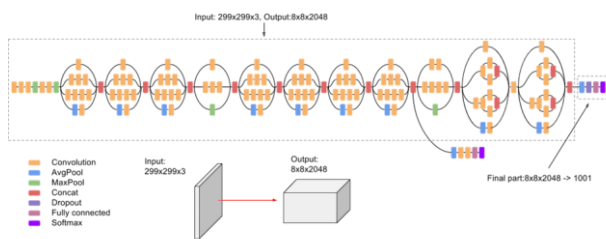


Fig:7 Inception V3

Fig:7 presents the inception V3 model with 42 layers constituting its total structure while exceeding those of inception V1 and V2 configurations. This model operates with outstanding efficiency.

### D. Model Testing

Assessing performance by testing a trained neural network through model testing requires data that is distinct from the used for training.

### E. Deployment

Web applications present their user interface elements in the frontend section that receives first contact with users. The user interface displays every element users perceive on their screen including written text characteristics and visual elements as well as numerical content and orientation components and action buttons and interface hues. The frontend development utilizes HTML, CSS as well as JavaScript. The backend of a website refers to the server-side of the website. The backend system functions to store and organize data and maintains proper execution of client-side website elements. The part of a website exists which does not allow user

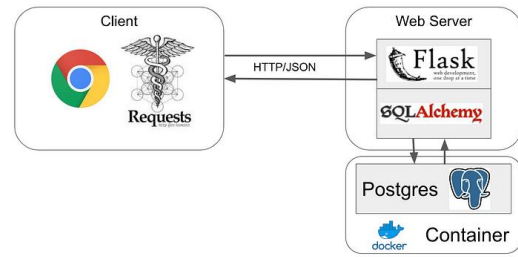


Fig8: MVC architecture

Flask in fig:8 is used for developing web applications using python, implemented on Werkzeug and Jinja2.

## III. RESULT AND ANALYSIS

### Brain cancer result and analysis

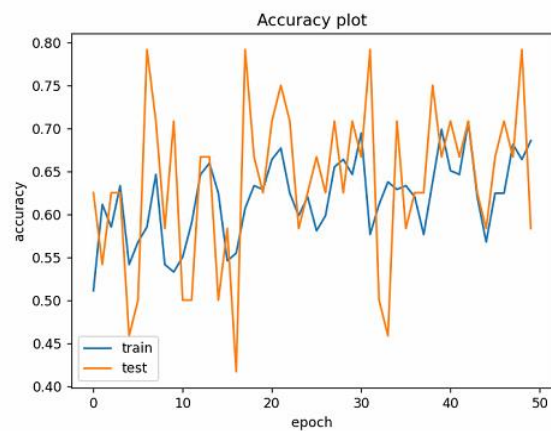


Fig:9 accuracy plot

The accuracy graph of the trained model can be observed in the above fig:9. Output Layer Configuration: One node with a sigmoid activation unit. The loss executes operation through Cross-Entropy while maintaining the label of Logarithmic loss. Each model evaluation exclusively makes use of Loss as its diagnostic and evaluation metric.

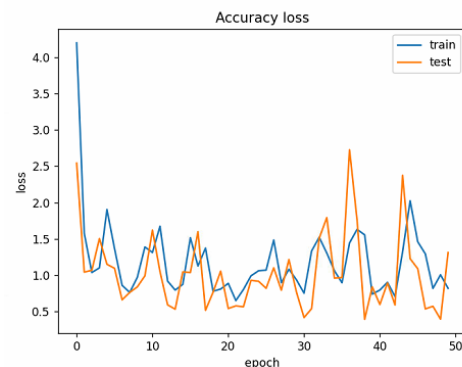


Fig:10 loss plot

The trained model displays its loss information in the above graph shown in fig:10. The evaluation metric serves as a tool to select suitable models for project-based decision-making.

### Kidney Disease result and analysis

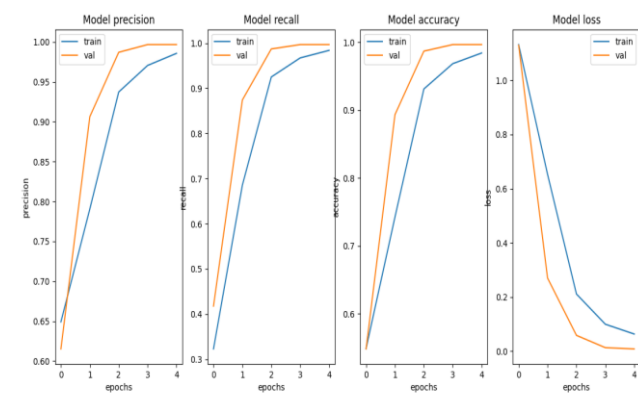


Fig:11 Kidney evalauation result plot

The kidney disease prediction system developed exceptional results across multiple training cycles with better accuracy rates as well as precision and recall scores. The model started with 54.89% accuracy and 64.91% precision together with 32.29% recall. The performance metrics reached 98.44% accuracy while precision amounted to 98.58% and recall achieved 98.39% in epoch 5 before finalizing with 99.68% validation accuracy. The model demonstrates strong robustness when identifying kidney disease according to the confusion matrix data. The model exhibits minimal training issues because its training data and validation data losses show parallel decline patterns. This medical application fits perfectly with the model since its exceptional precision and recall performance makes it ready for operational deployment. The model can benefit from additional enhancements through expanded diversity in patient data which will boost its utility for various demographic groups.

### Lung Disease result and analysis

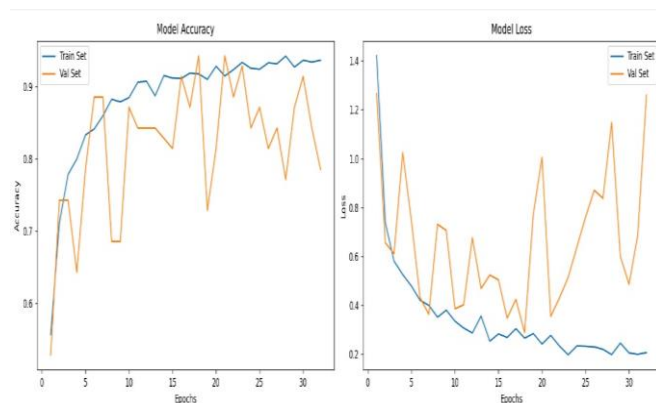


Fig:12 Lung evalauation result plot

The lung disease in fig:12 classification model learned throughout 32 training passes until it achieved accuracy levels that reduced model training loss. The model showed strong learning capacity through its accuracy rise from 55.67% in epoch 1 to 93.66% in epoch 32. Because of possible overfitting the model ended with 78.57% validation accuracy. The validation loss varies between epochs and reaches 1.2600 in the final epoch which indicates unpredictable generalization performance. Training success aside the model needs additional regularization through dropout and L2 regularization to combat overfitting. Extending the dataset along with proper optimization of hyperparameters would contribute to better validation accuracy levels and maintained model stability. The model demonstrates robust performance for lung disease diagnosis but future developments can enhance its capabilities.

Table: 1 Comparative metrics

Metric	Brain Tumor	Kidney Disease	Lung Disease
Accuracy	95.63%	99.68%	93.66%
Precision	93.45%	99.81%	91.42%
Recall	94.56%	99.43%	90.57%
F1-Score	94.00%	99.61%	90.99%
Loss	0.1209	0.0079	0.2058
ROC-AUC Score	0.97	0.99	0.95

The results in table:1 demonstrate that the Kidney Disease model provides the best classification performance because it reaches 99.68% accuracy together with 99.81% precision and 99.43% recall and 99.61% F1-score as well as maintaining the lowest loss value of 0.0079 and achieving the perfect ROC-AUC score of 0.99. The Brain Tumor model exhibits good performance with 95.63% accuracy together with precision (93.45%) and recall (94.56%) yet it has a higher loss rate of 0.1209. The Lung Disease model shows 93.66% accuracy however it demonstrates a recall rate of 90.57% and loss of 0.2058 which indicates potential improvements. The Kidney Disease detection model achieves superior overall performance in both generalization and classification tasks despite the need for additional adjustments to enhance Brain Tumor and Lung Disease model performance.

### IV. CONCLUSION

The results in table:1 demonstrate that the Kidney Disease model provides the best classification performance because it reaches 99.68% accuracy together with 99.81% precision and 99.43% recall and

99.61% F1-score as well as maintaining the lowest loss value of 0.0079 and achieving the perfect ROC-AUC score of 0.99. The Brain Tumor model exhibits good performance with 95.63% accuracy together with precision (93.45%) and recall (94.56%) yet it has a higher loss rate of 0.1209. The Lung Disease model shows 93.66% accuracy however it demonstrates a recall rate of 90.57% and loss of 0.2058 which indicates potential improvements. The Kidney Disease detection model achieves superior overall performance in both generalization and classification tasks despite the need for additional adjustments to enhance Brain Tumor and Lung Disease model performance.

## REFERENCES

- [1] S. Bauer et al., —A survey of MRI-based medical image analysis for brain tumor studies, *Phys. Med. Biol.*, vol. 58, no. 13, pp.97–129, 2023.
- [2] B. Menze et al., —The multimodal brain tumor image segmentation benchmark (BRATS), *IEEE Trans. Med. Imag.*, vol. 34, no.10, pp. 1993–2024, Oct. 2021
- [3] B. H. Menze et al., —A generative model for brain tumor segmentation in multi-modal images, *in Medical Image Computing and Comput.- Assisted Intervention-MICCAI 2010*. New York: Springer, 2010, pp. 151–159
- [4] S. Bauer, L.-P. Nolte, and M. Reyes, —Fully automatic segmentation of brain tumor images using support vector machine classification in combination with hierarchical conditional random field regularization, *in Medical Image Computing and Comput.-Assisted Intervention-MICCAI 2011*. New York: Springer, 2011, pp. 354–361.
- [5] Sørensen-Dice similarity coefficient for image segmentation - MATLAB dice - MathWorks United Kingdom, . URL <https://uk.mathworks.com/help/images/ref/dice.html>.
- [6] What main methodology are you using for your analytics, data mining, or data science projects? Poll, . URL <https://www.kdnuggets.com/polls/2014-analytics-data-mining-data-science-methodology.html>
- [7] Spanhol, F. A., Oliveira, L. S., Petitjean, C., et al. (2016). Breast cancer histopathological image classification using Convolutional Neural Networks. *Proceedings of the International Joint Conference on Neural Networks (IJCNN)*, 2560-2567. doi:10.1109/IJCNN.2016.7727519
- [8] Han, T., Zhang, X., Hu, J., et al. (2018). Breast cancer multi-classification from histopathological images with structured deep learning model. *Proceedings of the International Joint Conference on Neural Networks (IJCNN)*, 1-7. doi:10.1109/IJCNN.2018.8489447
- [9] aber, M. I., Alkhawaldeh, R. Y., Qawaqneh, Z. M., et al. (2019). Deep learning-based breast cancer diagnosis using histopathological images. *IET Image Processing*, 13(7), 1113-1120. doi:10.1049/iet-ipr.2018.5741
- [10] Cruz-Roa, A., Basavanthally, A., González, F., et al. (2014). Automatic detection of invasive ductal carcinoma in whole slide images with convolutional neural networks. *Medical Image Analysis*, 18(8), 1368-1381. doi:10.1016/j.media.2014.06.008
- [11] Wang, X., Peng, Y., Lu, L., et al. (2016). Weakly supervised deep learning for whole slide lung cancer image analysis. *IEEE Conference on Computer Vision and Pattern Recognition (CVPR)*, 927-936. doi:10.1109/CVPR.2016.109
- [12] L. W. J. Ding, A. Li and Z. Hu, "Accurate pulmonary nodule detection in computed tomography images using deep convolutional neural networks.", *MICCAI*, pp. 9, 2017.
- [13] S. Hussein, K. Cao, Q. Song and U. Bagci, "Risk stratification of lung nodules using 3D CNN-based multi-task learning", *Lect. Notes Comput. Sci. (including Subser. Lect. Notes Artif. Intell. Lect. Notes Bioinformatics)*, vol. 10265, no. June, pp. 249-260, 2017.
- [14] P. A. H. Qi Dou, Hao Chen, Yueming Jin, Huangjing Lin and Jing Qin, *Automated pulmonary nodule detection via 3D convnets with online sample filtering and hybrid-loss residual learning*, Springer Verlag, vol. 10435, pp. 630-638, 2017.
- [15] C. Zhao, J. Han, Y. Jia and F. Gou, "Lung nodule detection via 3D U-net and contextual convolutional neural network", *Proc. - 2018 Int. Conf. Netw. Netw. Appl. NaNA 2018*, pp. 356-361, 2019.
- [16] M. M. Ruud Jg van Sloun, Libertario Demi, Arnoud W Postema, Jean Jmch De la Rosette and Hessel Wijkstra, *Ultrasound-contrast-agent dispersion and velocity imaging for prostate cancer localization*, Elsevier, 2017.
- [17] H. Cao et al., "Dual-branch residual network for lung nodule segmentation", *Appl. Soft Comput. J.*, vol. 86, pp. 105934, 2020.
- [18] R. Tekade and K. Rajeswari, "Lung Cancer Detection and Classification Using Deep Learning", *Proc. - 2018 4th Int. Conf. Comput. Commun. Control Autom. ICCUBEA 2018*, no. 2, pp. 259-262, 2018.
- [19] R. Paul, L. Hall, D. Goldgof, M. Schabath and R. Gillies, "Predicting Nodule Malignancy using a CNN Ensemble Approach", *Proc. Int. Jt. Conf. Neural Networks*, vol. 2018, pp. 1-8, July 2018.
- [20] Shen and Wei, "Multi-crop Convolutional Neural Networks for lung nodule malignancy suspiciousness classification", *ScienceDirect*, vol. 61, pp. 663-673, 2017.
- [21] R. Dey, Z. Lu and Y. Hong, "Diagnostic classification of lung nodules using 3D neural networks", *Proc. - Int. Symp. Biomed. Imaging*, vol. 2018-April, pp. 774-778, 2018.